

Bandwidth Improvement of Compact Planar Antenna for UWB Application with Dual Notch Band Performance Using Parasitic Resonant Structure

Swarnaprava Sahoo*, Mihir N. Mohanty, and Laxmi P. Mishra

Abstract—This research article presents a compact planar antenna and a method for bandwidth improvement using parasitic resonant structure for UWB application with dual notch band performance, which are adjusted with an empirical formula. The radiating element of the microstrip square patch is slotted with two identical inverted J-shaped slots at the two non-radiating edges, a reversed F-shaped slot in the slotted radiating element, so that dual notch bands are excited. The bandwidth of the microstrip square patch radiator is improved with the help of a dumbbell-shaped parasitic resonant structure which is placed on the upper to partial ground plane for UWB application. The antenna, with size of $(12 \times 16 \text{ mm}^2)$, is fabricated on an epoxy FR-4 dielectric substrate of 1.6 mm thick and experimentally validated. The simulated and experimental results show that the invented radiator covers operating bandwidth from 2.8 to 13 GHz with $\text{VSWR} < 2$ and omnidirectional radiation characteristics. The two notch bands (3.3–4.2 and 5.1–5.4 GHz) are excited in the wide bandwidth by suppressing any interference from IEEE 802.16 WiMAX (3.3 GHz–3.6 GHz), C-band (3.7 GHz–4.2 GHz) and IEEE 802.11 a lower WLAN (5.15 GHz–5.482 GHz) with $\text{VSWR} > 5$.

1. INTRODUCTION

Due to compact size and ability of integration with other circuits and subsystems, modern wireless communication devices are most necessary. For such conventional devices, microstrip patch antenna is a proper choice due to light weight, easy fabrication, and inexpensive manufacturing. Narrow impedance bandwidth is the main drawback of a microstrip patch antenna. The frequency band from 3.1 GHz–10.6 GHz was assigned for ultra-wideband (UWB) communication of unlicensed use in 2002 by United States Federal Communications Commission (FCC) [1]. Hence, in recent years many researchers have concentrated on UWB antennas [2, 3]. Researchers are more interested in UWB communication system over the conventional wireless communication systems due to the popular advantages such as low price, compact size, easy fabrication, low manufacturing cost, high speed transmission data rate, low power dissipation, excellent immunity to multipath interference, reduced hardware complexity, and omnidirectional radiation characteristics across the whole bandwidth from 3.1–10.6 GHz [4–8]. UWB radiator is an important element in a UWB system with small size, proper performances and exempting interferences from near systems which are parts of the UWB spectrum. There are many existing narrowband services in UWB such as WiMAX and WLAN. Most Wi-MAX is operated in 3.3 GHz–3.8 GHz frequency band and WLAN in usually 5.15 GHz–5.825 GHz frequency band. Within a UWB system the potential electromagnetic interference is caused by these existing narrowbands. The interfering signals can be avoided with two possible ways. The first one is by using spatial filter like

Received 30 November 2017, Accepted 10 February 2018, Scheduled 21 March 2018

* Corresponding author: Swarnaprava Sahoo (swarna.sahoo@gmail.com).

The authors are with the Department of Electronics and Communication Engineering, Siksha 'O' Anusandhan (Deemed to be University), Bhubaneswar, Odisha, India.

frequency selective surface over the radiator [9]. However, this method is expensive and very spacious when it is integrated with other microwave circuitries. The second one uses radiators having filtering capable of frequency band of Wi-MAX (3.3 GHz–3.8 GHz) and WLAN (5.15 GHz–5.825 GHz). So, design of notched band radiators are very much important to notch the frequency band from 3.3 GHz–3.8 GHz and from 5.15 GHz–5.825 GHz in UWB range to prevent possible interference among UWB and existing Wi-MAX and WLAN systems, i.e., radiators with dual notch band performances. Other existing systems in the UWB range are IEEE 802.16 Wi-MAX (3.3 GHz to 3.6 GHz), C-band (3.7 GHz to 4.2 GHz) and IEEE 802.11a WLAN (5.15 GHz–5.825 GHz). To notch these systems, UWB antennas are required to preserve the UWB system and above said systems simultaneously from any interference among them. To overcome interference problems, many UWB antennas have been developed with different techniques using band-notch characteristics. They are single-layer differential CPW-fed tapered slot UWB radiators [10], by etching a semicircular annular parasitic strip above the radiating strip [11], by cutting a partial annular slot in the lower part of the ring radiator [12], by adding unsymmetrical split ring resonators [13], by inserting slots and slits [14]. The above said antennas can notch only single frequency band. Many UWB antenna designs are available in the literature with dual or triple notch bands characteristics, as listed in Table 2. They include parasitic elements in the radiating element, ground plane modifications and feed line modifications, by etching independent controllable strips, rectangular patch with two bevels, by cutting out two elliptic single complementary split-ring resonators (ESCSRs) from the radiating element of the radiator with two rectangular split ring resonators near the feed line patch junction of the radiator and by gluing padding patch [15–24]. Some of them are based on trial and error where a few designs are based on a systematic design [7, 8, 10, 12, 14, 18, 22]. As narrow impedance bandwidth is a shortcoming of the microstrip patch antenna, a method has been proposed to improve the impedance bandwidth.

In this article, a compact planar radiator is intended as well as a method for bandwidth improvement for UWB application with dual notch band characteristics that are adjusted with an empirical formula. By adjusting two identical inverted J-shaped slots in the non-radiating edge of the radiating element, the first notch band is introduced while the second notch band is achieved due to the inverted F-shaped slot inside the radiating element. The bandwidth is improved by dumbbell-shaped reared conductor plane. The compact radiator of dimension $12 \times 16 \text{ mm}^2$ is fabricated on an epoxy FR-4 dielectric substrate of 1.6 mm thick. The proposed antenna is simulated using HFSS, and for validation it is fabricated and measured. The intended radiator in this work attains notched band for IEEE 802.11a and has larger band width as well as more compact size than the reported radiators. The comparisons of dimension, notched band, bandwidth and gain of different UWB radiators with the present radiator are given in Table 2.

2. ANTENNA DESIGN

The radiating element is designed for UWB range (3.1 GHz–10.6 GHz) on an epoxy FR-4 dielectric substrate shown in Fig. 1. The dimension of microstrip square patch is $\lambda_g/2 \times \lambda_g/2$, where $\lambda_g = c/f_c\sqrt{\epsilon_r}$, c = velocity of light = 3×10^8 m/sec, ϵ_r = dielectric constant of the substrate = 4.4, and f_c = centre frequency = 6.85 GHz. The proposed radiator is fed by a microstrip line of size $5.9 \times 2 \text{ mm}^2$ for 50 ohm impedance matching. All the optimized dimensions of the intended radiator are listed in Table 1.

The antenna dimensions can be deduced from analytical expressions [25].

(a) Effective Dielectric Constant:

$$\epsilon_{reff} = \frac{\epsilon_r + 1}{2} + \frac{\epsilon_r - 1}{2 \left(1 + 12 \frac{h}{W}\right)} = 3.3 \quad (1)$$

(b) Patch length:

$$L_{\text{patch}} = \frac{c}{2f_0\sqrt{\epsilon_{reff}}} - 2\Delta L = 10 \text{ mm} \quad (2)$$

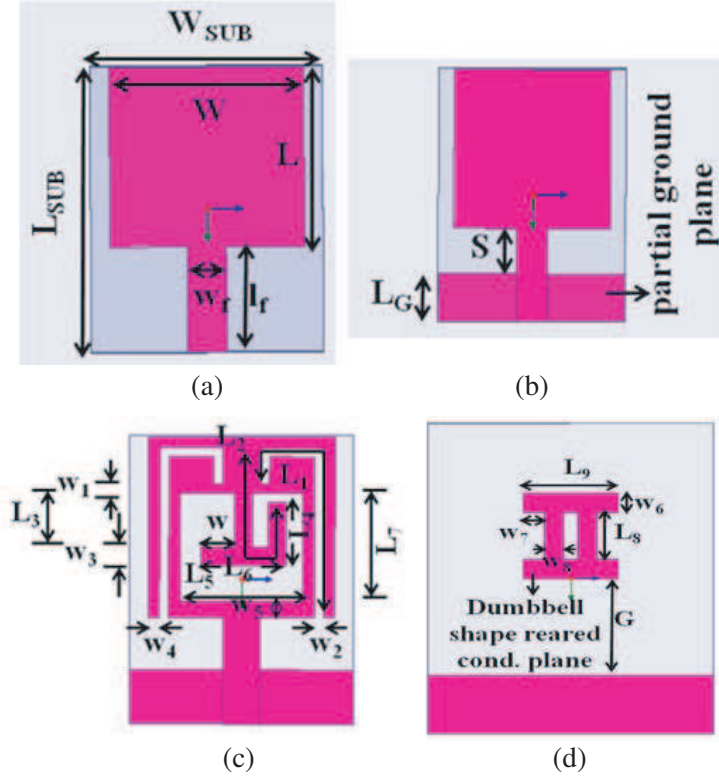


Figure 1. Design of proposed radiator, (a) initial microstrip square patch antenna (antenna 1), (b) microstrip square patch radiator with partial ground plane (radiator 2), (c) slotted microstrip square patch radiator with partial ground plane (antenna 3), (d) slotted microstrip square patch antenna with reared conductor plane (proposed antenna) (antenna 4).

(c) The change in length due to fringing effects:

$$\Delta L = 0.412h \frac{(\epsilon_{eff} + 0.3) \left(\frac{W_{patch}}{h} + 0.264 \right)}{(\epsilon_{reff} - 0.258) \left(\frac{W_{patch}}{h} + 0.8 \right)} = 0.72 \text{ mm} \quad (3)$$

(d) Width of patch,

$$W_{patch} = \frac{c}{2f_r} \sqrt{\frac{2}{\epsilon_r + 1}} = 10 \text{ mm} \quad (4)$$

The HFSS software is used for antenna design, parametric analysis and optimization. The substrate is taken as FR-4 epoxy with dielectric constant 4.4 (ϵ_r), loss tangent 0.02 ($\tan \delta$) and thickness 1.6 mm (h). The optimized partial ground plane is taken as 3.4 mm \times 12 mm.

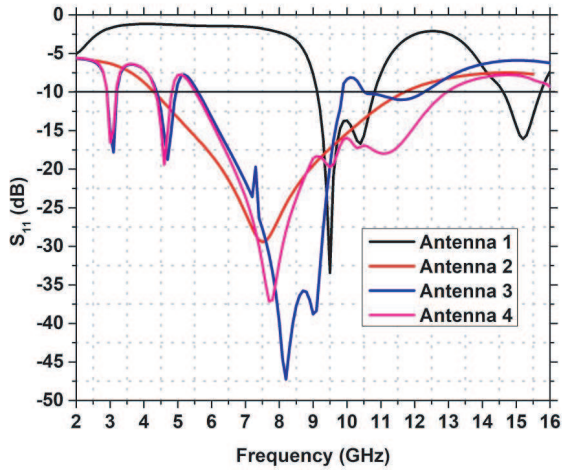
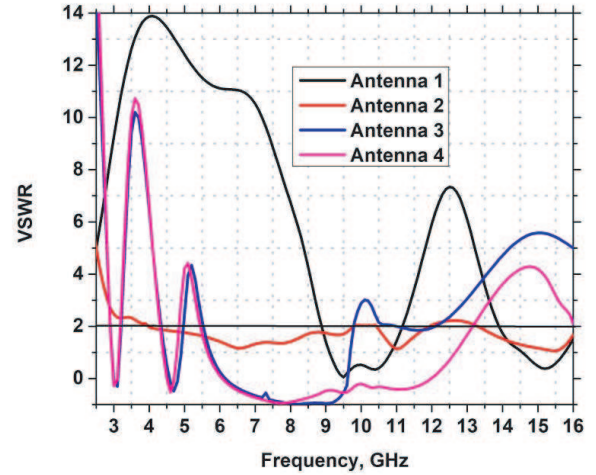
The optimized partial ground plane is taken as 3.4 mm \times 12 mm. The metallic patch and partial ground plane is separated by 2.95 mm which is the optimum gap. The microstrip square radiating element is slotted such that the antenna creates two notch bands which modify the performance of the radiator. The two notch bands are at Wi-MAX (from 3.3 to 3.6 GHz), C-band (from 3.7 to 4.2 GHz) and lower WLAN (from 5.1 to 5.4 GHz). A dumbbell-shaped parasitic resonant structure is inserted above the partial ground plane which is bottom layer of the dielectric substrate for bandwidth enhancement as shown in Fig. 1(d). The structure is symmetrically placed in respect of the longitudinal direction of the radiator. The size of dumbbell-shaped structure is optimized for better performance at 9.5 GHz and above frequencies, which does not affect the lower band performance of the radiator. Table 1 gives the optimized dimensions of the dumbbell-shaped structure.

Table 1. The optimized dimensions of the intended radiator.

Parameters	Value (mm)	Parameters	Value (mm)	Parameters	Value (mm)
W	10	L_2	12.3	w_3	1.2
L	10	L_3	3	w_4	0.6
L_{SUB}	16	L_4	3.7	w_5	1
W_{SUB}	12	L_5	4.6	w_6	1
w_f	2	L_6	6.6	w_7	0.9
l_f	5.9	L_7	6	w_8	0.8
L_G	3.4	w	1.6	G	5.2
S	2.95	w_1	0.5	L_8	2.4
L_1	14.8	w_2	0.5	L_9	4

3. RESULTS AND DISCUSSION

Figure 2 presents the simulated return loss graph of the four antennas. The separation between the radiating element and partial ground plane increases which increases the impedance bandwidth because of extra electromagnetic coupling in between radiating element and the partial ground plane.

**Figure 2.** Simulated return loss graph.**Figure 3.** Simulated VSWR plot.

The VSWR plot of the microstrip square patch radiator with partial ground plane is given in Fig. 3 which covers bandwidth from 4.4 to 11.7 GHz with VSWR < 2.

Figure 1(c) shows the slotted microstrip square patch radiator with partial ground plane. At the non-radiating edge of the square patch, two identical inverted J-shaped slots are inserted which creates the first notch band centered at 3.7 GHz. Another notched band is excited due to inverted F-shaped slot inside the radiating element centered at 5.2 GHz. The centre of notch bands (f_1 and f_2) is related with parameters (L_1 and L_2) as [12, 26]:

$$L_1 \cong \frac{c}{3.1f_1\sqrt{\epsilon_{reff}}} \quad (5)$$

$$L_2 \cong \frac{c}{2.5f_2\sqrt{\epsilon_{reff}}} \quad (6)$$

where, L_1 denotes slot length of mirror inverted J-shaped slot which defines the first notched band, and L_2 denotes the slot length of inverted F-shaped slot inside the radiating element which defines the second notched band. The parameters L_1 and L_2 can be evaluated from Equations (5) and (6) as 14.3 mm and 12.7 mm for the notched band centre frequency at 3.7 and 5.2 GHz. Fig. 1(c) shows the optimized parameters of the proposed radiator based on the calculated values of L_1 and L_2 using HFSS software. Fig. 3 shows that radiator 3 covers bandwidth from 2.8 GHz to 9.8 GHz with voltage standing wave ratio < 2 . The first notch band is centered at 3.7 GHz with $VSWR > 10$ while the second notch band is centered at 5.2 GHz with $VSWR > 4$. Here the antenna has poor performance in UWB range. This performance can be overcome by UWB frequency range. Since the UWB frequency varies up to 10.6 GHz, the frequency band of the antenna can vary from 9.8 to 10.6 GHz or above 10.6 GHz. The parasitic resonant structure placed on the rear side of the dielectric substrate acts as a dipole that provides the additional coupling path. Again the inductance and capacitance values of the input impedance are changed due to this structure which helps to increase the impedance bandwidth. The bandwidth is improved significantly between the bands 9.8 and 13 GHz without affecting the lower band performance of the antenna. The intended radiator attains a bandwidth from 2.8–13 GHz ($VSWR < 2$). The antenna parameters L_1 and L_2 are calculated using HFSS software which satisfies Equations (5) and (6). The simulated results are presented in Fig. 4 and Fig. 5.

Parameter L_1 specifies the first notch band, and parameter L_2 specifies the second notch band. The simulation generated results are presented in Fig. 4 and Fig. 5 by putting dielectric constant $\epsilon_{r\text{eff}} = 3.3$ (calculated from Equation (1)) and antenna parameters L_1, L_2 in Equations (5) and (6), and the centre frequencies f_1 and f_2 of the notch bands calculated from Equations (5) and (6) satisfy the simulation results presented in Fig. 4 and Fig. 5.

Figure 6 gives a clear explanation of the physical meaning of generation of notch band by inserting inverted J- and F-shaped slots and the surface current distribution along with calculation of frequency at the centre of two notch bands using High Frequency Structure Simulator within the pass band.

Figure 6(a) shows that at 3.7 GHz the surface current distributions at the edges of the two inverted J-shaped slots are opposite in direction, so that the total efficient radiation is very low that helps to introduce the first notch band. Fig. 6(b) shows that at 5.2 GHz, the direction of surface current distribution in inverted F-shaped slot is opposite in direction to the current direction in external edge of the radiator. Hence, at this frequency the entire radiation is limited, and the second notch band is introduced. Fig. 6(c) gives the surface current distribution at 9.5 GHz, and the entire structure acts as a radiator apart from the notch bands. The direction of current is same at individual parts of the radiator, so that an efficient radiation appears.

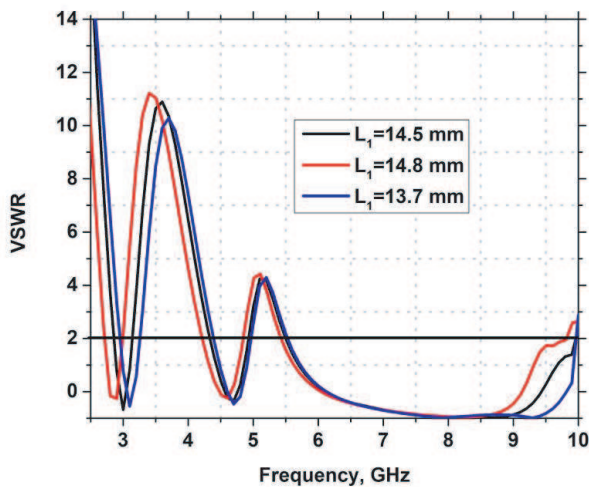


Figure 4. Simulation VSWR plot of the intended radiator for various L_1 .

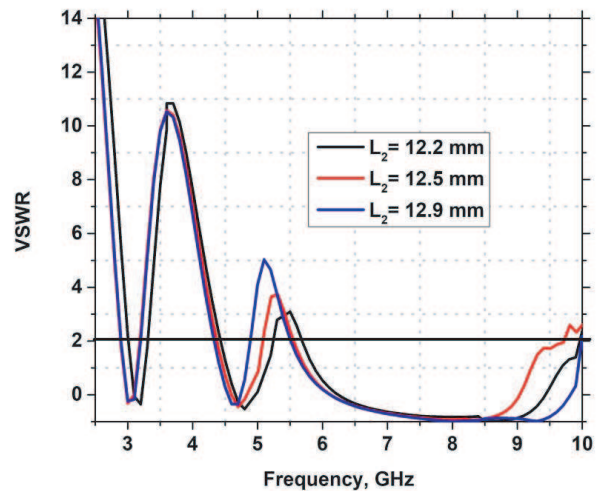


Figure 5. Simulation VSWR plot of the intended radiator for various L_2 .

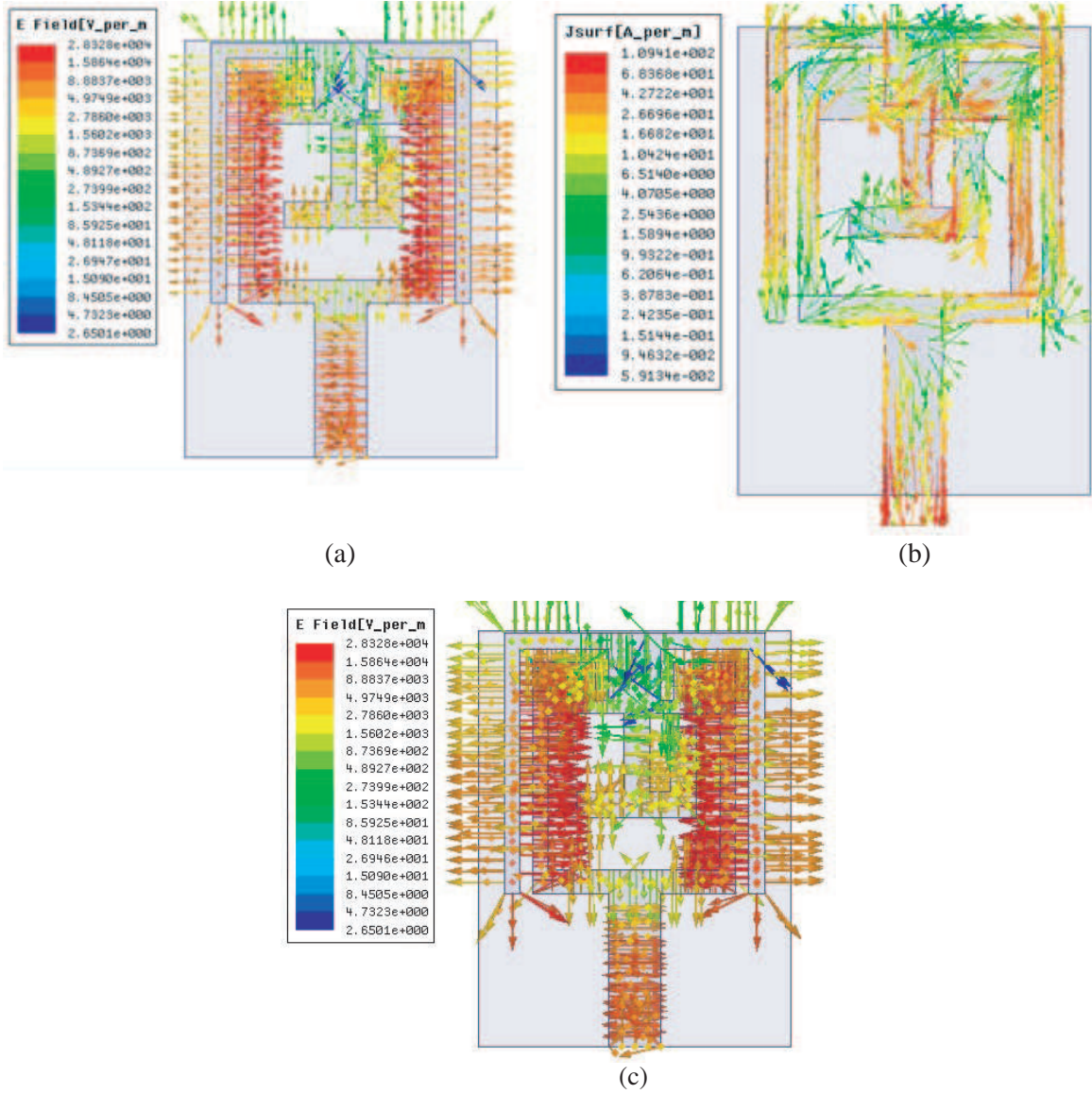


Figure 6. Simulated surface current distribution of the intended radiator at (a) 3.7 GHz, (b) 5.2 GHz and (c) 9.5 GHz.

The proposed antenna of size $W_{\text{SUB}} \times L_{\text{SUB}} = 12 \times 16 \text{ mm}^2$ has been validated using an Agilent N5247A VNA, and the radiation characteristics are validated in an anechoic chamber and a rotation table with signal generator antenna measurement system. Photographs of antenna prototype are shown in Fig. 11. To get perfect measurement characteristics of the proposed antenna is the main problem as in other small antennas. This problem is due to the connection of coaxial cable between measured antenna and vector network analyzer. If it is not coupled perfectly, then the measurement cable will become some parts of the radiator, hence there is some change in input impedance of the radiator. Fig. 7 presents the simulated and measured VSWR plots of the intended radiator.

Figure 7 indicates that the impedance bandwidth of the intended radiator varies from 2.8–13 GHz except two notch bands (3.3–4.2 and 5.1–5.4 GHz). Basically the simulated and experimental results are in good contract. Another key element of UWB performance of the antenna is group delay which is verified by measuring the group delay variation over the whole band. The group delay is the time domain characteristics of UWB radiator, which indicates the phase distortion during transmission [27].

Mathematically,

$$\text{Group delay, } \tau = -\frac{d\phi(\omega)}{d(\omega)} = -\frac{1}{2\pi} \frac{d\phi(f)}{d(f)} \text{ where, } \omega \text{ is angular frequency.}$$

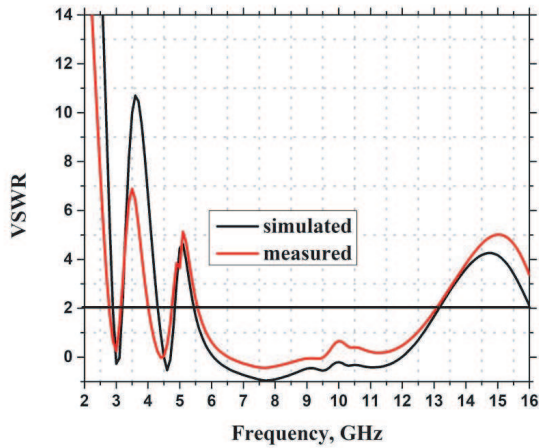


Figure 7. Simulated and experimental VSWR of the intended dual notch band monopole radiator.

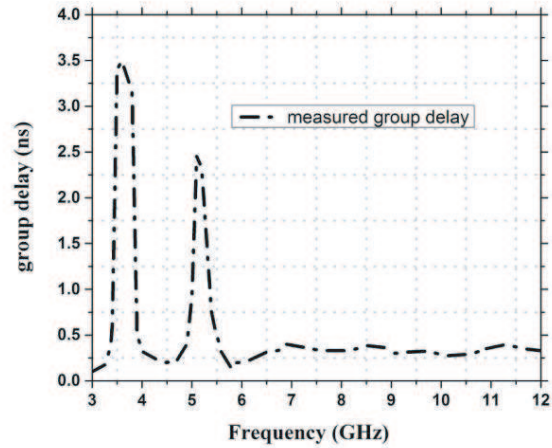
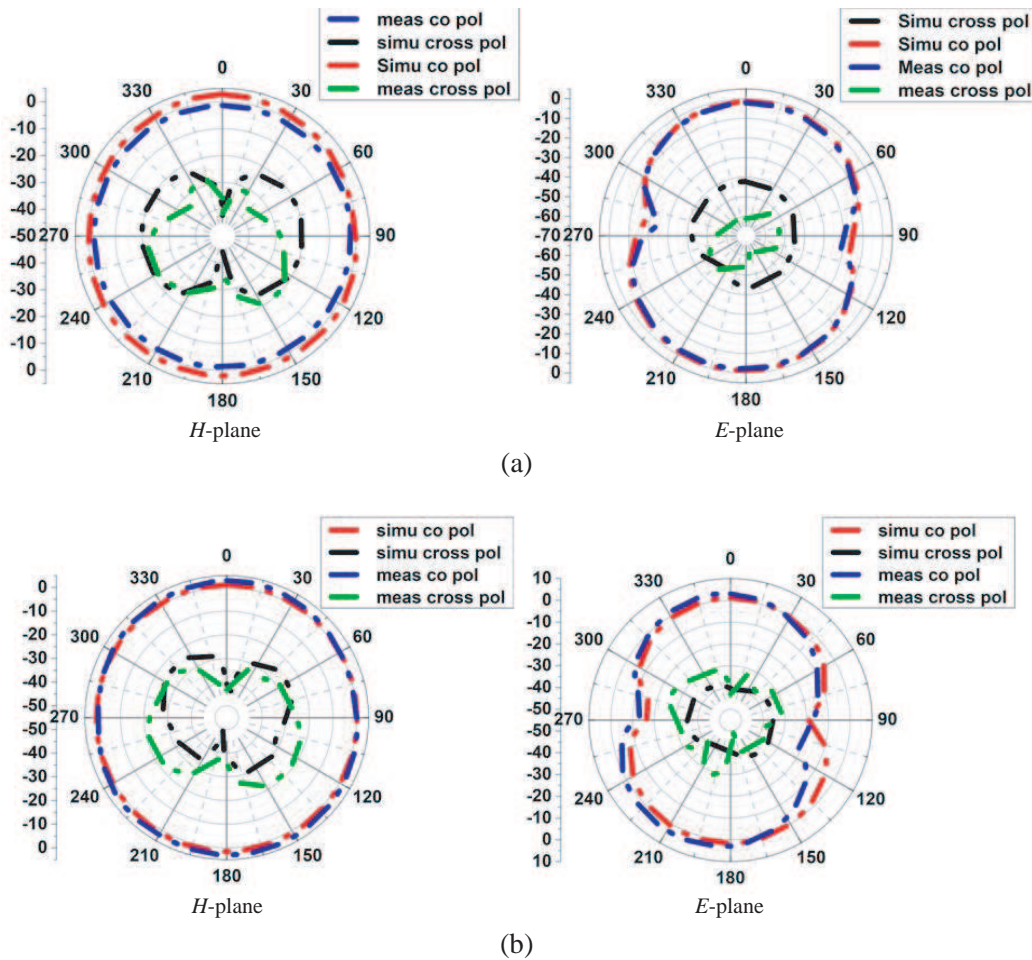


Figure 8. Measured group delay of the proposed antenna.



(a)

(b)

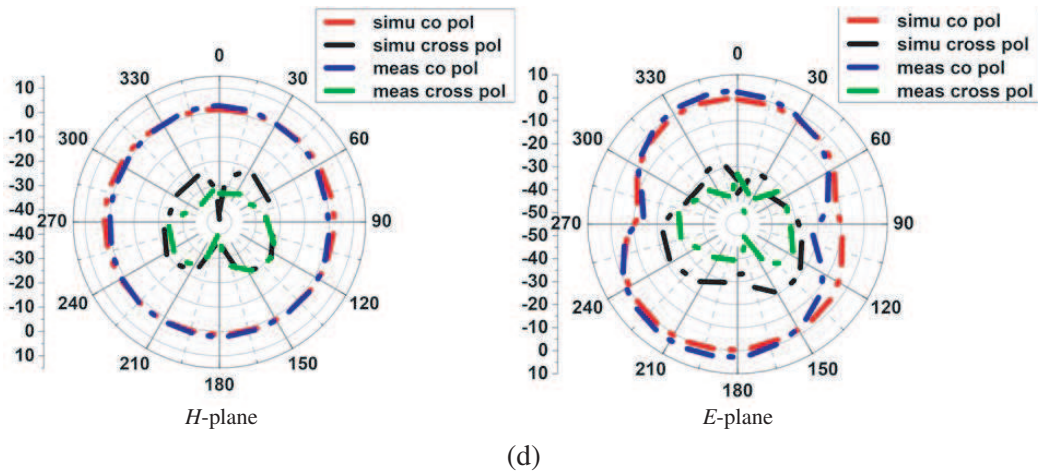
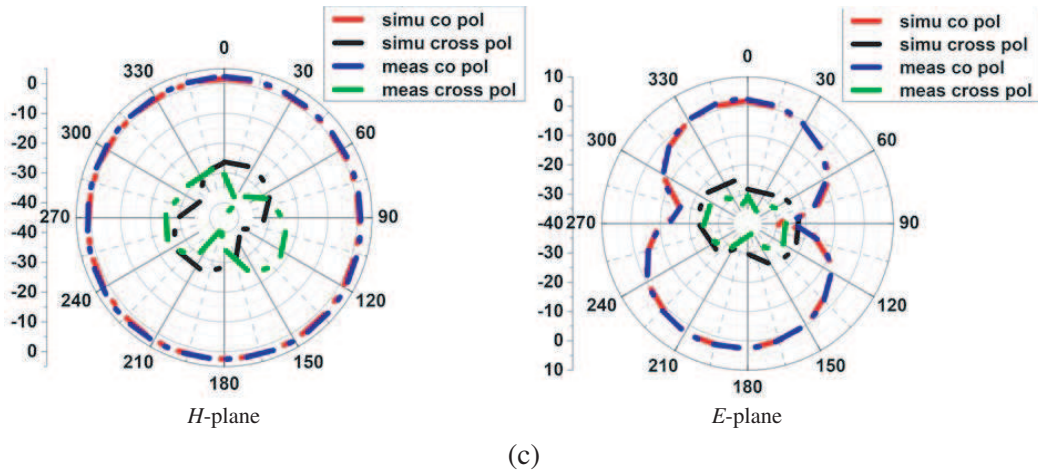


Figure 9. Simulated and experimental radiation characteristics of the intended dual notch band monopole radiator at (a) 3 GHz, (b) 4.6 GHz, (c) 7.7 GHz and (d) 9.5 GHz.

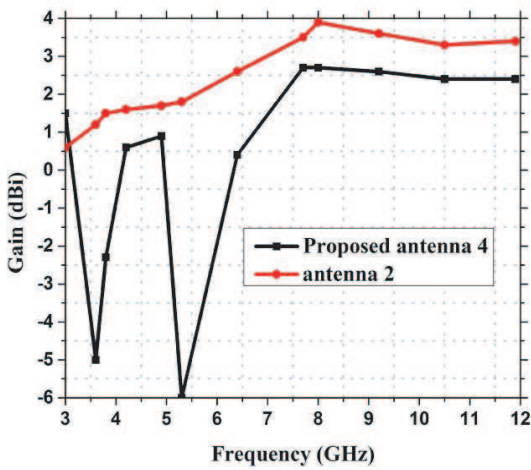


Figure 10. Measured gain comparison between the proposed antenna and microstrip square patch radiator with truncated ground plane (antenna 2).

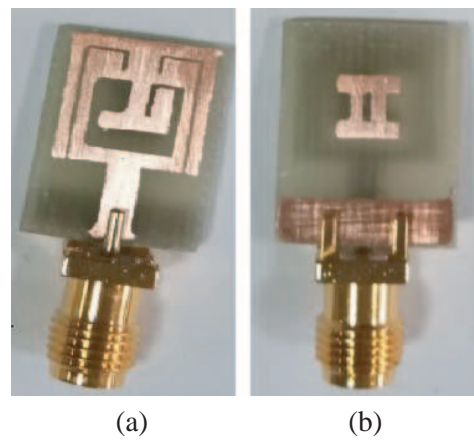


Figure 11. Photograph of radiator prototype, (a) front side, (b) back side.

The variation of group delay should be very small in passband for less distortion performance. The group delay of the proposed radiator has been measured in between transmitter and receiver antennas kept apart at a distance of 10 cm in broad side direction facing to each other. The measured group delay is shown in Fig. 8.

Figure 8 shows that the group delay varies from 0.1 to 0.5 ns in passband but up to 3.5 ns in notch band. Fig. 9 shows the simulated and experimental radiation characteristics of the intended radiator H and E -planes at frequencies 3, 4.6, 7.7 and 9.5 GHz, respectively.

Basically in H - and E -planes, the radiation characteristics are almost omnidirectional and closely directional (Fig. 8 shape), respectively for lower and middle frequency bands. The cross polarization level is below -20 dB across the whole impedance bandwidth. Overall, the radiation patterns are stable and symmetrical. The reflected part into the field among the under test and reference radiators may cause a small discrimination in radiation patterns.

Figure 10 displays the measured gain of the intended radiator from 3 GHz to 12 GHz which is compared with the gain of microstrip square patch radiator with partial ground plane (radiator 2). The plot confirms the effects of the utilized procedure in the desertion of two notch bands. Again the dual band notched radiator attains smooth gain excluding the two notched bands. The gain drops rapidly

Table 2. Comparison of previous band notched UWB antennas with present antenna.

Band notch UWB antennas	Dimensions (mm ³)	Notched band (GHz)	Bandwidth (GHz)	Max. Gain (dBi)	Area (mm ²)
[8]	27 × 20 × 0.64	4–6 (HIPERLAN/2)	2.7–10 (8.7 GHz)	4.6	540
[10]	30 × 28 × 1	5.2–6 (WLAN)	2.78–12.3 (9.52 GHz)	2.87	840
[11]	28 × 27 × 1.6	5.1–5.8 (WLAN)	2.99–12 (9.01 GHz)	2.35	756
[12]	26 × 24 × 0.5	5.1–5.95 (WLAN, DSRC)	3–10.6 (7.6 GHz)	4.8	624
[13]	26 × 24 × 1.53	5.05–5.9 (WLAN)	3.65–11 (7.35 GHz)	6.85	624
[14]	39 × 35 × 0.7	5–6 (WLAN)	3.1–10.6 (7.5 GHz)	3	1365
[15]	10 × 16 × 1.6	3.47–4.3 (WiMAX), 5.1–5.95 (WLAN)	2.89–10.83 (7.94 GHz)	5	160
[18]	25 × 25.5 × 0.508	5–6, 4–7, 4.5–5.5, 6.5–7.5, 8.5–9.5	3–11 (8 GHz)	3.9	637.5
[20]	19.5 × 21 × 1	5.15–5.85 (WLAN), 3.3–3.6 (WiMAX), 3.7–4.2 (C-band)	2.6–11 (8.4 GHz)	2	409.5
[21]	44 × 38 × 1.57	5.35–5.8 (WLAN), 7.98–8.85 (ITU)	2.9–10.9 (8 GHz)	3.2	1672
[22]	24 × 36 × 1.524	5.15–5.35 (lower WLAN), 5.725–5.825 (Upper WLAN)	3–11 (8 GHz)	4.2	864
[23]	31 × 20 × 0.8	3.3–3.7 (WiMAX), 5.15–5.85 (WLAN), 7.1–7.76 (X band downlink satellite comm.)	3.1–11 (7.9 GHz)	2.9	620
[24]	35 × 35 × 1.6	3.3–3.8 (WiMAX), 5.15–5.85 (WLAN), 7.9–8.4 (X band)	2.21–11.71 (9.5 GHz)	5.2	1225
Proposed antenna	12 × 16 × 1.6	3.3–3.6 (WiMAX), 3.7–4.2 (C-band), 5.15–5.482 (lower WLAN)	2.8–13 (10.2 GHz)	2.6	192

at the two notch bands. The characteristics mentioned above show clearly that the intended radiator is the best choice for UWB applications which need to obstruct any interfering wireless systems such as Wi-MAX (3.3 GHz–3.6 GHz), C-band (3.7 GHz–4.2 GHz) and lower WLAN (5.1 GHz–5.4 GHz).

4. CONCLUSION

A compact microstrip line fed monopole planar radiator has been suggested for UWB application and dual notch band performance with bandwidth enhancement using a parasitic resonant structure. The square radiating element of the intended radiator is in slotted form and parasitic resonant structure with truncated ground plane. Based on empirical formulas, two notch bands are created at the desired frequencies with appropriate slot dimensions. The first notch band is attained by inserting two identical inverted J-shaped slots in the radiating element that prevents interference in UWB system such as WiMAX and C-band systems that are exempted from interferences. The second notch is obtained by inserting inverted an F-shaped slot which is stretched in centre of the slotted radiating element that prevents the interference with 5 GHz lower WLAN systems. Again for bandwidth improvement, a dumbbell (II) shaped parasitic resonant structure is used with proper dimensions. The impedance bandwidth (129.11%) of the intended radiator varies from 2.8 GHz to 13 GHz with two notched bands centered at 3.7 GHz and

ACKNOWLEDGMENT

We are very much thankful to Mr. Raja Ram Prasad of Indian Institute of Technology, Roorkee, India for fabrication and testing of this work.

REFERENCES

1. “Federal Communications Commission revision of Part 15 of the Commission’s rules regarding ultra-wideband transmission system from 3.1 to 10.6 GHz,” ET-Docket, 98–153, FEDERAL Communications Commission (FCC), Washington, DC, 2002.
2. Foudazi, A., H. R. Hassani, and S. M. A. Nezhad, “Small UWB planar monopole antenna with added GPS/GSM/WLAN bands,” *IEEE Transactions on Antennas and Propagation*, Vol. 60, No. 6, 2987–2992, 2012.
3. Tsai, C. L. and C. L. Yang, “Novel compact eye shaped UWB antennas,” *IEEE Antennas and Wireless Propagation Letters*, Vol. 11, 184–187, 2012.
4. Moosazadeh, M., C. Ghobadi, and M. Dousti, “Small monopole antenna with checkered shaped patch for UWB application,” *IEEE Antennas and Wireless Propagation Letters*, Vol. 9, 1014–1017, 2010.
5. Gorla, H. R. and F. J. Harackiewicz, “Dual-three stepped trident ultra-wideband planar monopole antenna,” *Progress In Electromagnetics Research C*, Vol. 69, 19–26, 2016.
6. Fereidoony, F., S. Chamanni, and S. A. Mirtaheri, “Systematic design of UWB monopole antennas with stable omnidirectional radiation pattern,” *IEEE Antennas and Wireless Propagation Letters*, Vol. 11, 752–755, 2012.
7. Samal, P. B., P. J. Soh, and G. A. E. Vandenbosch, “A systematic design procedure for microstrip-based unidirectional UWB antennas,” *Progress In Electromagnetics Research*, Vol. 143, 105–130, 2013.
8. Abbosh, A. M., M. E. Bialkowski, J. Mazierska, and M. V. Jacob, “A planar UWB antenna with signal rejection capability in the 4–6 GHz band,” *IEEE Microwave and Wireless Components Letters*, Vol. 16, No. 5, 278–280, 2006.
9. Yeo, J. and R. Mittra, “A novel wideband antenna package design with a compact spatial notch filter for wireless applications,” *Microwave and Optical Technology Letters*, Vol. 35, No. 6, 455–460, 2002.

10. Tu, Z. H., W. A. Li, and Q. X. Chu, "Single layer differential CPW fed notch band tapered slot UWB antenna," *IEEE Antennas and Wireless Propagation Letters*, Vol. 13, 1296–1299, 2014.
11. Azim, R., A. T. Mobashsher, and M. T. Islam, "UWB band notch antenna with a semicircular annular strip," *Trends in Applied Sciences Research*, Vol. 6, No. 9, 1078–1084, 2011.
12. Azim, R. and M. T. Islam, "Compact planar UWB antenna with band notch characteristics for WLAN and DSRC," *Progress In Electromagnetics Research*, Vol. 133, 391–406, 2013.
13. Gorla, H. R. and F. J. Harackiewicz, "Dual trident UWB planar antenna with band notch for WLAN," *Progress In Electromagnetics Research Letters*, Vol. 54, 115–121, 2015.
14. Yazdi, M. and N. Komjani, "A compact band-notched UWB planar monopole antenna with parasitic elements," *Progress In Electromagnetics Research Letters*, Vol. 24, 129–138, 2011.
15. Mehranpour, M., J. Nourinia, C. Ghobadi, and M. Ojaroudi, "Dual band notched square monopole antenna for ultra wideband applications," *IEEE Antennas and Wireless Propagation Letters*, Vol. 11, 172–175, 2012.
16. Mahmud, M. Z., M. T. Islam, and M. Samsuzzaman, "A high performance UWB antenna design for microwave imaging system," *Microwave and Optical Technology Letters*, Vol. 58, No. 8, 1824–1831, 2016.
17. Hossain, M. J., M. R. I. Faruque, and M. T. Islam, "Design of a patch antenna for ultra wideband applications," *Microwave and Optical Technology Letters*, Vol. 58, No. 9, 2152–2156, 2016.
18. Abbosh, A. M. and M. E. Bialkowski, "Design of UWB planar band notched antenna using parasitic elements," *IEEE Transactions on Antennas and Propagation*, Vol. 57, No. 3, 796–799, 2009.
19. Aissaoui, D., L. M. Abdelghani, B. Hacem, and T. A. Denodni, "CPW fed UWB hexagonal shaped antenna with additional fractal elements," *Microwave and Optical Technology Letters*, Vol. 58, No. 10, 2370–2374, 2016.
20. Azarmanesh, M., S. Soltani, and P. Lotfi, "Design of an ultra wide band monopole antenna with WiMAX, C and wireless local area network band notches," *IET Microwave, Antennas and Propagation*, Vol. 5, No. 6, 728–733, 2011.
21. Koohestani, M., N. Pires, A. K. Skrivervik, and A. A. Moreira, "Band reject ultra wide band monopole antenna using patch loading," *Electronics Letters*, Vol. 48, No. 16, 974–975, 2012.
22. Ryu, K. S. and A. A. Kishk, "UWB antenna with single or dual band-notches for lower WLAN band and upper WLAN band," *IEEE Transactions on Antennas and Propagation*, Vol. 57, No. 12, 3942–3950, 2009.
23. Bakariya, P. S., S. Dwari, and M. Sarkari, "A triple band notch compact UWB printed monopole antenna," *Wireless Personal Communication*, Vol. 82, No. 2, 1095–1106, 2015.
24. Sarkar, D., K. V. Srivastava, and K. Saurav, "A compact microstrip fed triple band notched UWB monopole antenna," *IEEE Antennas and Wireless Propagation Letters*, Vol. 13, 396–399, 2014.
25. Balanis, C. A., *Antenna Theory, Analysis and Design*, 2nd Edition, John Wiley & Sons, 2005.
26. Gupta, K., R. Garg, I. Bahl, and P. Bhartia, *Microstrip Lines and Slot Lines*, 2nd Edition, Artech House, 1996.
27. Krishna, R. V. S. R. and R. Kumar, "A slotted UWB monopole antenna with single port and double ports for dual polarization," *Engineering Science and Technology an International Journal*, Vol. 19, No. 1, 470–484, 2016.